# Vacancy clusters in ultrafine grained Al by severe plastic deformation

X. L. Wu[a)]
*State Key Laboratory of Nonlinear Mechanics, Institute of Mechanics, Chinese Academy of Sciences, Beijing 100080, China*

B. Li and E. Ma[b)]
*Department of Materials Science and Engineering, Johns Hopkins University, Baltimore, Maryland 21218, USA*

(Received 10 August 2007; accepted 15 September 2007; published online 2 October 2007)

Bulk nanostructured metals are often formed via severe plastic deformation (SPD). The dislocations generated during SPD evolve into boundaries to decompose the grains. Vacancies are also produced in large numbers during SPD, but have received much less attention. Using transmission electron microscopy, here we demonstrate a high density of unusually large vacancy Frank loops in SPD-processed Al. They are shown to impede moving dislocations and should be a contributor to strength. © *2007 American Institute of Physics*. [DOI: 10.1063/1.2794416]

Bulk ultrafine-grained (UFG) and nanostructured (NS) metals are often prepared via severe plastic deformation (SPD),[1,2] which refines the originally large grains. The high-angle and low-angle grain boundaries (GBs), as well as the subgrain dislocation structures stored, are usually taken as the only microstructural features responsible for the macroscopic strength/ductility properties of the UFG/NS metal obtained. However, SPD also introduces into the material another nanoscale feature in large numbers. That is, the aggregates of point defects generated throughout the SPD process.[3,4] For example, the movement of a screw dislocation with a jog should result in the creation of a row of either interstitial atoms or vacancies.[3] The vacancies are dominant because the energy to form a vacancy is smaller than that to form an interstitial. A high density of vacancies is expected for SPD, because of the intense dislocation interactions and tremendous plastic strain characteristic of SPD. The vacancy population present during and after SPD depends on the deformation rate, SPD route, temperature, etc.

Point defect clusters are known to be very important in controlling the strength, toughness, and stability (such as swelling) of irradiated (nuclear) metals and alloys.[5–7] For point defects produced via deformation, evidence for vacancy concentration of the order of $10^{-4}$, close to the equilibrium value at the melting temperature ($T_m$), has been provided by differential scanning calorimetry, electrical resistivity measurements, and x-ray Bragg profile analysis.[8,9] However, the nanoscale entities formed by vacancies and their effects on the properties of the SPD-processed UFG/NS metals have not drawn adequate attention. For example, the stacking faults (SFs) observed in UFG/NS metals have all been attributed to dislocation dissociation or partial dislocation emission.[10] Little consideration is given to the vacancy clusters that may form SFs. It is therefore the goal of this letter to call attention to these vacancy-type defects produced by SPD. Their size, density, thermal stability, and effects on strength will be evaluated in the following using Al as an example.

High-purity Al (99.999%) specimens were subjected to equal channel angular pressing (ECAP) for four passes (true shear strain of ~4) via route $B_C$ at room temperature (RT). No storage of vacancy-type clusters was observed in the transmission electron microscopy (TEM) after such ECAP. This is because for a metal like Al with relatively low $T_m$, RT is a sufficiently high temperature for dynamic recovery during ECAP to change the defect structures. SPD of other metals are often done at RT, or $< \sim 0.2T_m$. To deform Al at such low homologous temperature, 1-mm-thick sheets were cut from the ECAP sample for additional rolling to 70% strain, through ~16 passes each at a strain rate of $\sim 10^{-2}$ $s^{-1}$, with liquid nitrogen (LN) cooling between consecutive rolling passes (120 and 150 K before and after each pass). The processed specimens were kept in LN. The microstructure including the vacancy clusters[11] was observed at RT in a TEM operating at 120 kV. The hardness of the samples was measured by averaging >12 indentations using an instrumented MTS Nano Indenter$^{XP}$ at a constant loading rate to an indentation depth of 2 $\mu$m.

After ECAP+LN rolling, the (~25 $\mu$m thick) Al can be categorized as in the UFG regime,[1] with a predominantly lamellar microstructure (not shown) containing a high population of dislocations. The thickness of the elongated grains spans a fairly wide range from ~200 to 800 nm. Equiaxed grains are also observed sometimes. The GBs are mostly of the high-angle types.

Our focus is the vacancy clusters inside the grain interior. Figure 1(a) is a weak-beam dark-field (WBDF) image, taken using diffraction condition $\mathbf{g}(5\mathbf{g})$, $\mathbf{g}=200$, in an orientation close to the [110] zone axis. One observes a high density of very small bright spots, each of which comes from the local strain field produced by a cluster of vacancies due to depth-dependent variations in diffraction contrast.[12] An enlarged view is shown in the inset. These near-round-shaped entities are vacancy Frank loops, rather than stacking fault tetrahedra (SFTs) that would appear either triangle shaped or square shaped under the same diffraction conditions.[11,13] Figure 1(b) is a further enlarged view of the loops in a region near the GB. When a loop intersects with a (111) plane, a straight trace is formed. These traces on two different {111}-type planes are observed, as marked with arrows. A lattice image of one trace is shown in Fig. 1(c). The straight red line indicates lattice shift due to the presence of a SF, relative to the parallel reference blue line. This confirms further that what is observed here is vacancy Frank loop, leading to a SF.

[a)]Electronic mail: xlwu@imech.ac.cn
[b)]Electronic mail: ema@jhu.edu

 

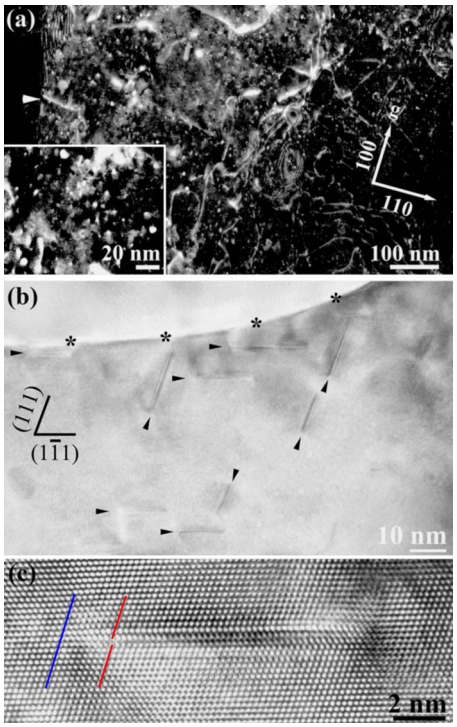


FIG. 1. (Color online) (a) WBDF micrograph showing faulted dislocation loops (bright spots) in Al. The inset is an enlarged view. The arrow marks the GB. Note the presence of dislocations. (b) SFs indicated by arrows near the GB (asterisks). (c) Lattice image of a SF of ~8 nm long.

Inspections of Fig. 1 and a large number of TEM images indicate that the vacancy Frank loops range from 2 nm to as large as 18 nm in diameter.

Also, the SFs are observed to be close-by to one another, indicating a high volume density. These clusters are stable, in the absence of dynamic recovery, and remained nearly unchanged after aging for 1 month at RT. In comparison, some moderate annealing at 373 K for 30 min eliminated almost all the SFs.

The SFs observed above in the grain interior are clearly not due to the dissociation of dislocations. For the latter (the core of a common $1/2\langle 110\rangle$ type edge dislocations split into two $1/6\langle 112\rangle$ Shockley partial dislocations, connected by a SF), the splitting distance of the extended dislocation, $r_s$, depends on the stacking fault energy $\gamma$ and the applied stress $\sigma$ as[14]

$$r_s = Kb^2/(\gamma - bm\sigma), \tag{1}$$

where $b$ is the length of the Burgers vector of the partials, $K$ is a factor that depends on the elastic constants of the material, and $m$ is the Schmid factor. $r_s$ can be enlarged under the high $\sigma$ required to deform NS metals, but Al has a very high $\gamma$. In molecular dynamics (MD) simulations, Yamakov *et al.*[15] obtained the SF width of only 0.86 nm for the dissociation of a 60° $1/2\langle 011\rangle$ dislocation, and Bulatov *et al.*[16] obtained a similar value of 1.01 nm. The dissociation of a perfect screw dislocation in Al was calculated to give an extremely narrow SF (~0.28 nm).[17] In experiments, a combination of high resolution TEM observations and image simulations concluded that the 60° dislocations were slightly dissociated, with a narrow width of 0.55 nm.[18] The SF widths observed here (up to 18 nm) are clearly well beyond all these findings and would not be consistent with predictions based on energy considerations. The only claim of wide SFs in Al was after ball milling.[19,20] However, some of their SFs are right at the GBs (Ref. 19) and can be formed by the GB emission of partial dislocations.[10,21]

Deformation-induced vacancies[7–9] migrate and coalesce to form microscopic clusters, lowering the free energy of a system containing supersaturated point defects. A vacancy cluster continues to grow to become a vacancy Frank loop by absorbing more vacancies, further lowering energy. The faulted loop on (111) planes is, in fact, the predicted morphology/configuration in continuum elastic energy calculations to be the most stable for small Al clusters (e.g., $<\sim 1000$ vacancies).[22] The transition between faulted and perfect loops in Al occurs at a loop diameter of $\leqslant 15$ nm (2500 vacancies), overcoming an energy barrier for the unfaulting process.[23] The loop sizes in our Al are generally below this size, and these loops are therefore expected to be faulted ones, consistent with all previous reports for quenching or irradiation by electron, ion, or neutron. The noteworthy feature here, however, is that after SPD we have large vacancy Frank loops (as large as 18 nm) with a high volume density.

Such vacancy Frank loops on the slip plane have consequences in affecting dislocation motion,[24] which remains to be understood for SPD metals. We have performed MD simulations using the embedded atom method potential for Al,[25] in a system with approximately $1\times 10^6$ atoms. The time step was 3 fs. Free surfaces were applied in all directions to avoid the effect that a periodic boundary condition can impose on dislocation glide. Two vacancy-type loops 6 nm in diameter ($2r$) were introduced, together with a moving dislocation. The center-to-center distance $L$ was taken to be 16 nm as an extreme case (the experimental $L$ values are larger but of the same order of magnitude). By sorting out the atoms with different coordination numbers from that of the perfect lattice, the interaction process between the loops and the moving dislocation core can be visualized and monitored.

The system was relaxed first. The original loops were seen to take the form of incomplete SFTs,[26] as shown in Fig. 2(a). Due to the high $\gamma$, fully developed SFTs were not formed. The dislocation was dissociated into two partials as expected: $1/2[\bar{1}01]\rightarrow 1/6[\bar{2}11]+\mathrm{SF}\ (\sim 1\ \mathrm{nm})+1/6[\bar{1}\bar{1}2]$. When a shear strain was applied (the MD shear strain rate was $4.8\times 10^8$/s), the dislocation moved to approach the loops. Figure 2 clearly reveals that the loops have strong pinning effect on the dislocation. The dislocation segments that were not pinned by the loops kept gliding forward, leading to bowing of the dislocation line in between the two loops. The pinned segments of the dislocation were virtually immobile on the slip plane, until later cross slip as the alternative route by gliding on other intercepting {111} planes, in an effort to get over the faulted regions (incomplete SFT) above the loops. Such cross slip demands higher stresses and creates jogs with low mobility along the way (see Fig. 2).

The energy barrier that the slip must overcome can be assessed using the generalized SF energy,[10] calculated by displacing part of the crystal along the $1/2\langle 112\rangle$ direction on a {111} plane. For an ideal lattice, an energy valley appears at a displacement of about 1/3 (in the unit of the $x$ axis in Fig. 3), and this is the well-known pathway for a unit dislocation ($1/2\langle 110\rangle$) to dissociate into partials with $b=1/6\langle 112\rangle$ type

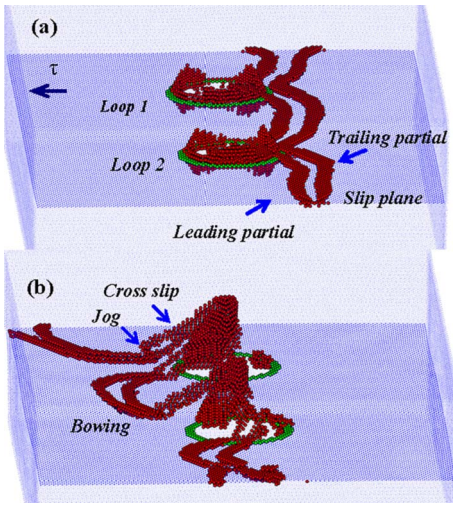


FIG. 2. (Color online) Three-dimensional visualization of interactions between two vacancy Frank loops (SFs) and a moving dislocation. (a) On the highlighted slip plane, the dislocation dissociates into two partials under the high stresses. (b) Bowing out of the dislocations when they are blocked and pinned down by the loops. Cross slip occurred as the pinned segments moved to above the original slip plane over the faulted region, also generating immobile jogs in the dislocation path.

to glide in directions with lower-energy barrier. Figure 3 also illustrates the energy penalty when vacancy Frank loops with different sizes are introduced to the slip plane. When $r$ is very small at 2 nm, the energy barrier remains almost the same, and the dislocations cut through in our simulations. However, the energy barrier increases at larger loop sizes. At 6 nm and above, there is, in fact, no displacement in Fig. 3 that would enable the crossing of a barrier to allow a downhill process and a lower-energy configuration. Instead, dislocation moving in this direction cutting through the loop would never be over the hump, with ever-increasing energy penalty. This is why the segments running into the SFs are effectively blocked, requiring costly cross slip (Fig. 2) to get around the obstacles.

One could view this pinning effect as similar to the precipitate strengthening process in Al alloys, where the incoming dislocation also bows out in between the pinning points (nondeforming precipitates). Higher stresses are needed for this process to happen that lengthens the dislocation line and increases its curvature. Under such an idealized model scenario, the strengthening effect would be of the order of

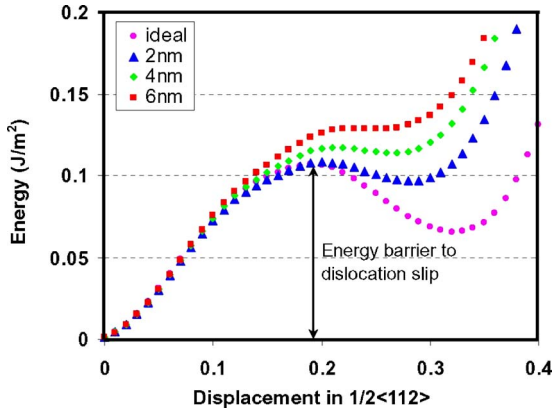


FIG. 3. (Color online) Generalized stacking fault energies when vacancy Frank loops of different sizes were introduced on the slip plane, showing the energy barrier to dislocation slip. See text.

$G/100$ or 260 MPa, from the stress needed to force the dislocation between the obstacles,

$$\tau_B = \frac{Gb}{L-2r}, \tag{2}$$

where $G$ is the shear modulus. Experimentally, LN rolling elevated the hardness from 380 to 520 MPa (there was, however, increase in dislocation density inevitably concurrent with the retention of the loops). In any case, one should take into account the role of vacancy Frank loops when discussing the high strength of SPD metals, because $r$ is unusually large here (effective blocking/pinning of dislocations) and $L$ is small (high obstacle density). For other metals with higher $T_m$, such vacancy clusters resulting in SFs are likely to be present after SPD at RT. In addition to strengthening, such large and dense defects may also affect other mechanical properties of SPD nanomaterials, opening up a subject for future research.

X.L.W. acknowledges NSFC (50471086 and 50571110), the 973 Program (2004CB619305), the CAS (KJCX2-YW-M04), and the Innovation Program. B.L. and E.M. are supported at JHU by US NSF (DMR-0355395), and at CAMCS by ARMAC-RTP (DAAD19-01-2-0003 and W911NF-06-2-0006).

[1]R. Z. Valiev and T. G. Langdon, Prog. Mater. Sci. **51**, 881 (2006).
[2]D. Jia, Y. Wang, K. T. Ramesh, E. Ma, Y. T. Zhu, and R. Valiev, Appl. Phys. Lett. **79**, 611 (2001).
[3]R. E. Reed Hill and R. Abbaschian, *Physical Metallurgy Principle*, 3rd ed. (PWS, Boston, 1991), p. 853.
[4]J. Schiøtz, T. Leffers, and B. N. Singh, Philos. Mag. Lett. **81**, 301 (2001).
[5]M. Kiritani, J. Nucl. Mater. **212-215**, 192 (1986).
[6]M. Victoria, N. Baluc, C. Bailat, Y. Dai, M. I. Luppo, R. Schaublin, and B. N. Singh, J. Nucl. Mater. **276**, 114 (2000).
[7]N. M. Ghoniem, B. N. Singh, L. Z. Sun, and T. D. de la Rubia, J. Nucl. Mater. **276**, 166 (2000).
[8]M. J. Zehetbauer, G. Steiner, E. Schafler, A. Korznikov, and E. Korznikova, Mater. Sci. Forum **503-504**, 57 (2006).
[9]K. Detemple, O. Kanert, J. Th. M. De Hosson, and K. L. Murty, Phys. Rev. B **52**, 125 (1995).
[10]H. Van Swygenhoven, P. M. Derlet, and A. G. Frøseth, Acta Mater. **54**, 1975 (2006).
[11]M. Kiritani, Y. Satoh, Y. Kizuka, K. Arakawa, Y. Ogasawara, S. Arai, and Y. Shimomura, Philos. Mag. Lett. **79**, 797 (1999).
[12]R. Schäublin, A. Almazouzi, Y. Dai, Y. N. Osetsky, and M. Victoria, J. Nucl. Mater. **276**, 251 (2000).
[13]Y. Satoh, H. Taoka, S. Komima, Y. Yoshiie, and M. Kiritani, Philos. Mag. A **70**, 869 (1994).
[14]J. P. Hirth and J. Lothe, *Theory of Dislocations* (Wiley, New York, 1982), Chap. 10–3, pp. 313–353.
[15]V. Yamakov, D. Wolf, M. Salazar, S. R. Phillpot, and H. Gleiter, Acta Mater. **49**, 2713 (2001).
[16]V. V. Bulatov, O. Richmond, and M. V. Glazov, Acta Mater. **47**, 3507 (1999).
[17]D. M. Esterling, Acta Metall. **28**, 1287 (1980).
[18]M. J. Mills and P. Stadelmann, Philos. Mag. A **60**, 355 (1989).
[19]X. Z. Liao, F. Zhou, E. J. Lavernia, S. G. Srinivasan, M. I. Baskes, D. W. He, and Y. T. Zhu, Appl. Phys. Lett. **83**, 632 (2003).
[20]S. G. Srinivasan, X. Z. Liao, M. I. Baskes, R. J. McCabe, Y. H. Zhao, and Y. T. Zhu, Phys. Rev. Lett. **94**, 125502 (2005).
[21]M. W. Chen, E. Ma, K. J. Hemker, H. W. Sheng, Y. M. Wang, and X. Cheng, Science **300**, 1275 (2003).
[22]S. J. Zinkle, L. E. Seitzman, and W. G. Wolfer, Philos. Mag. A **55**, 111 (1987).
[23]S. G. Song, J. I. Cole, and S. M. Bruemmer, Acta Mater. **45**, 501 (1997).
[24]M. Hiratani, V. V. Bulatov, and H. M. Zbib, J. Nucl. Mater. **329-333**, 1103 (2004).
[25]A. F. Voter and S. P. Chen, *MRS Symposia Proceeding* (Materials Research Society, Pittsburgh, 1987), Vol. 82, p. 175.
[26]T. Kadoyoshi, H. Kaburaki, F. Shimizu, H. Kimizuka, S. Jitsukawa, and J. Li, Acta Mater. **55**, 3073 (2007).